

# Symplastic Intercellular Connectivity Regulates Lateral Root Patterning

Yoselin Benitez-Alfonso,<sup>1,3,\*</sup> Christine Faulkner,<sup>1,4</sup> Ali Pendle,<sup>1</sup> Shunsuke Miyashima,<sup>2</sup> Ykä Helariutta,<sup>2</sup> and Andrew Maule<sup>1</sup>

<sup>1</sup>John Innes Centre, Norwich Research Park, Norwich, Norfolk NR4 7UH, UK

<sup>2</sup>Institute of Biotechnology/Department of Biosciences, University of Helsinki, Helsinki FI-00014, Finland

<sup>3</sup>Present address: Centre for Plant Sciences, School of Biology, University of Leeds, Leeds LS2 9JT, UK

<sup>4</sup>Present address: Department of Biological and Medical Sciences, Oxford Brookes University, Gypsy Lane, Oxford OX3 0BP, UK

\*Correspondence: [y.benitez-alfonso@leeds.ac.uk](mailto:y.benitez-alfonso@leeds.ac.uk)

<http://dx.doi.org/10.1016/j.devcel.2013.06.010>

This is an open-access article distributed under the terms of the Creative Commons Attribution-NonCommercial-No Derivative Works License, which permits non-commercial use, distribution, and reproduction in any medium, provided the original author and source are credited.

## SUMMARY

Cell-to-cell communication coordinates the behavior of individual cells to establish organ patterning and development. Although mobile signals are known to be important in lateral root development, the role of plasmodesmata (PD)-mediated transport in this process has not been investigated. Here, we show that changes in symplastic connectivity accompany and regulate lateral root organogenesis in *Arabidopsis*. This connectivity is dependent upon callose deposition around PD affecting molecular flux through the channel. Two plasmodesmal-localized  $\beta$ -1,3 glucanases (PdBGs) were identified that regulate callose accumulation and the number and distribution of lateral roots. The fundamental role of PD-associated callose in this process was illustrated by the induction of similar phenotypes in lines with altered callose turnover. Our results show that regulation of callose and cell-to-cell connectivity is critical in determining the pattern of lateral root formation, which influences root architecture and optimal plant performance.

## INTRODUCTION

The initiation of lateral root primordia (LRP) characterizes post-embryonic root development. This process uses environmental information to specify the relative positioning of primordia in order to maximize the potential for nutrient uptake. Lateral root emergence and extension then delivers an increase in root functional capacity underpinning increased plant growth (Péret et al., 2009; De Smet et al., 2006; Benková and Bielach, 2010).

The molecular mechanisms that determine lateral root (LR) architecture have significant agronomic relevance but remain poorly understood. Different from the primary root meristem, secondary meristems are initiated de novo from xylem-pole pericycle (XPP) cells in the differentiation zone of the primary root. This process involves multiple steps of cellular redefinition and cell proliferation that have been classified into seven stages

(I to VII) (Malamy and Benfey, 1997). Interconnected signaling pathways involving both hormone (auxin/cytokinin) transport and auxin/indole-3-acetic acid proteins (Aux/IAA) have been shown to regulate the expression of genes required during specification, dedifferentiation and emergence of the lateral meristems (Aloni et al., 2006; De Rybel et al., 2010; De Smet et al., 2010; Lucas et al., 2008; Moreira et al., 2013; Van Norman et al., 2011; Muraro et al., 2013). Oscillating auxin maxima in the basal meristem and, presumably, the intercellular transport of other mobile signals (Van Norman et al., 2011; De Smet et al., 2010; Moreno-Risueno et al., 2010) determines the characteristic spatial patterning of LRs, i.e., a regular distribution along the main root axis, oriented left-right in an alternating pattern.

The intercellular symplastic movement of signaling molecules through plasmodesmata (PD) determines embryonic cell fate and postembryonic organ development (Xu et al., 2011; Xu and Jackson, 2010; Kim et al., 2002; Nakajima et al., 2001). Regulation of PD transport can be controlled through the accumulation of the  $\beta$ -1,3 glucan callose in the surrounding wall causing a constriction of the symplastic channel (Zavaliev et al., 2011). Callose turnover at PDs affects both targeted molecular transport (dependent on proteins and cofactors capable of modifying PD aperture) and nontargeted molecular flux (diffusion of small molecules such as GFP) (Vatén et al., 2011; Rinne et al., 2011; Guseman et al., 2010; Benitez-Alfonso et al., 2009). This regulatory mechanism plays a key role in a plethora of developmental processes including the specification of stomatal complexes, dormancy release prior to flowering, the maintenance of apical meristems, and during the sink-source transition (Guseman et al., 2010; Levy et al., 2007b; Vatén et al., 2011; Rinne et al., 2011). It also regulates plant responses to biotic and abiotic stresses (Benitez-Alfonso et al., 2009, 2011; Levy et al., 2007a; Lee et al., 2011). In spite of the evidence that PD are dynamic structures and crucial to plant development and responses, our understanding of the mechanics of PD function remains poor. Recently, significant progress has been made in the identification of novel PD proteins through genetic or proteomic screens (Bayer et al., 2006; Fernandez-Calvino et al., 2011; Simpson et al., 2009; Thomas et al., 2008; Vatén et al., 2011). These studies have identified proteins involved directly in callose synthesis and degradation (callose synthases [CALS] and  $\beta$ -1,3 glucanases [BG]) or indirectly modifying callose

deposition (e.g., PD-callose binding protein [PDCB]) as PD components (Vatén et al., 2011; Fernandez-Calvino et al., 2011; Levy et al., 2007a; Simpson et al., 2009).

The importance of mobile factors (hormones, peptides, miRNAs, etc.) in lateral root initiation and emergence is well recognized (De Smet et al., 2008, 2010; Marin et al., 2010; Meng et al., 2012; Moreno-Risueno et al., 2010; Péret et al., 2012). It has been shown that misregulated PD connectivity, affecting the movement of non-cell-autonomous factors and the downstream processes they trigger, can have a negative impact on the development of apical meristems and meristemooids (Guseman et al., 2010; Benitez-Alfonso et al., 2009; Kim et al., 2003; Nakajima et al., 2001; Rinne et al., 2011; Van Norman et al., 2011; Vatén et al., 2011; Xu et al., 2011). However, the role of symplastic transport in the formation of lateral root meristems has not yet been investigated. In this article, we show that symplastic connectivity is critical for both the initiation and positioning of LR meristems and that this connectivity is regulated by PD-associated glucanases concomitant with callose as a regulator of symplastic molecular flux through PD.

## RESULTS

### Symplastic Connectivity Is Regulated during Lateral Root Development

To address the temporal and spatial regulation of cell-to-cell connectivity during primordia development, we used stable transgenic lines expressing reporters for GFP diffusion. For the purpose of this study, we divided mature roots into three main regions: meristem (where cell division occurs), basal meristem (from the end of cell division to the first root hair, containing the region of LR priming), and lateral root forming zone (LR forming zone; containing stages I–VII and emerged primordia as defined in other publications) (Figure 1A) (Malamy and Benfey, 1997). GFP expressed under the control of the *sucrose-proton symporter 2* (*SUC2*) promoter (active in phloem companion cells) (Truernit and Sauer, 1995) diffuses freely across all cell layers in the meristem (Stadler et al., 2005; Benitez-Alfonso et al., 2009). In the basal meristem and early LR forming region of 6-day-old roots, we detected GFP signal in the stele, endodermis, cortex, and epidermis suggesting that symplastic connectivity between the phloem and the outer cell layers is maintained in this region (Figure 1B). In contrast, GFP movement was differentially regulated in the LR forming zone (Figures 1C–1G). Proximal to stage II and III primordia, GFP movement was reduced but still diffused to pericycle cells, into the primordium and the endodermis (Figures 1C and 1D). However, p*SUC2*-expressed GFP was excluded from stage IV–V primordia (notice that diffusion is still detectable in neighboring pericycle cells; Figures 1E and 1F) and fluorescent signal in the new LR was only restored when a new functional vascular system was formed (Figure 1G).

The results from the analysis of p*SUC2*-GFP plants suggest a block in postphloem symplastic transport in late stages of primordia development; however, molecules produced within the primordium might have a different fate. To investigate this aspect, we generated transgenic plants expressing cytoplasmic GFP under the control of the *AUX1* promoter. We first confirmed *AUX1* expression in the basal meristem and LR

forming zone using a translational fluorescent fusion. As described previously (Marchant et al., 2002), *AUX1* expression in the stele of the basal meristem zone gets restricted to the new LRP in the LR forming zone (Figures S1M–S1R available online). Analysis of transgenic Col-0 plants, expressing p*AUX1*-GFP, confirmed stage IV and older LRP as domains with restricted connectivity to external cells. As for p*SUC2*-GFP, free GFP diffuses from the stele into the surrounding tissue in the basal meristem zone (compare Figures S1M and 1H). Similarly, GFP produced in stage I–III primordia diffuses to neighboring tissues and cortical cells (Figure 1I). However, GFP produced in stage IV and older primordia was retained within the primordium (Figures 1J–1L). Emerged primordia resembled the expression and diffusion profile of the main meristem (Figures 1M and S1S).

Together, these data point to a dynamic regulation of symplastic transport whereby positive cell-to-cell connectivity between pericycle cells and early stage primordia and the surrounding tissue becomes restricted in older LRP until emergence is completed.

### Callose Deposition at PD Correlates with the Formation of Symplastic Domains in Lateral Roots

Symplastic transport is regulated by the synthesis and degradation of callose at PD neck regions (Levy et al., 2007b; Vatén et al., 2011). This mechanism has been found to be important in the maintenance of symplastic permeability in apical meristems (Chen et al., 2009; Zavaliev et al., 2011; Benitez-Alfonso et al., 2009; Vatén et al., 2011). Therefore, we analyzed the pattern of callose deposition during the formation of lateral meristems. Whole roots, excised from Col-0 seedling 6 days postgermination (dpg), were fixed and immunolabeled with callose antibodies. Secondary detection with the fluorophore Alexa 488 revealed that callose is deposited in the sieve plates, cell plates, and in a punctate pattern in the cell wall, reminiscent of PD localization (Figures 2A–2G). The analysis of multiple root sections revealed differences in the level of callose accumulated in the basal meristem and LR forming zones. Callose deposition was detected at low levels at PDs of the basal meristem zone and in nonlateral root regions within the LR forming zone (Figure 2A). At early stages of lateral root development, callose gets deposited in the cell-plates and to moderate levels between cell layers (Figures 2B and 2C). In contrast, in stage IV–V primordia PD and cell wall labeling between the new meristem, the associated endodermal/cortical cell layer and the vasculature was significantly increased (Figures 2D and 2E). This is coincident with the reduction in GFP diffusion observed in p*SUC2*-GFP and p*AUX1*-GFP plants (Figures 1E, 1F, and 1J–1L). In the later stages, and during emergence, callose accumulation decreased but was still detected in the ruptured cortical and epidermal cells and in the new division walls within the new LR (Figures 2F and 2G). To quantify these changes in callose accumulation, we stained a significant number (>20) of wild-type roots with the callose stain aniline blue and calculated the mean increment in fluorescence signal (mean gray value) in the cell wall connecting the new lateral root and the overlying tissue (Figure S2). This mean gray value was corrected by subtracting the background fluorescence contained in the same area in the wall opposite the primordium. The results support our previous conclusions,

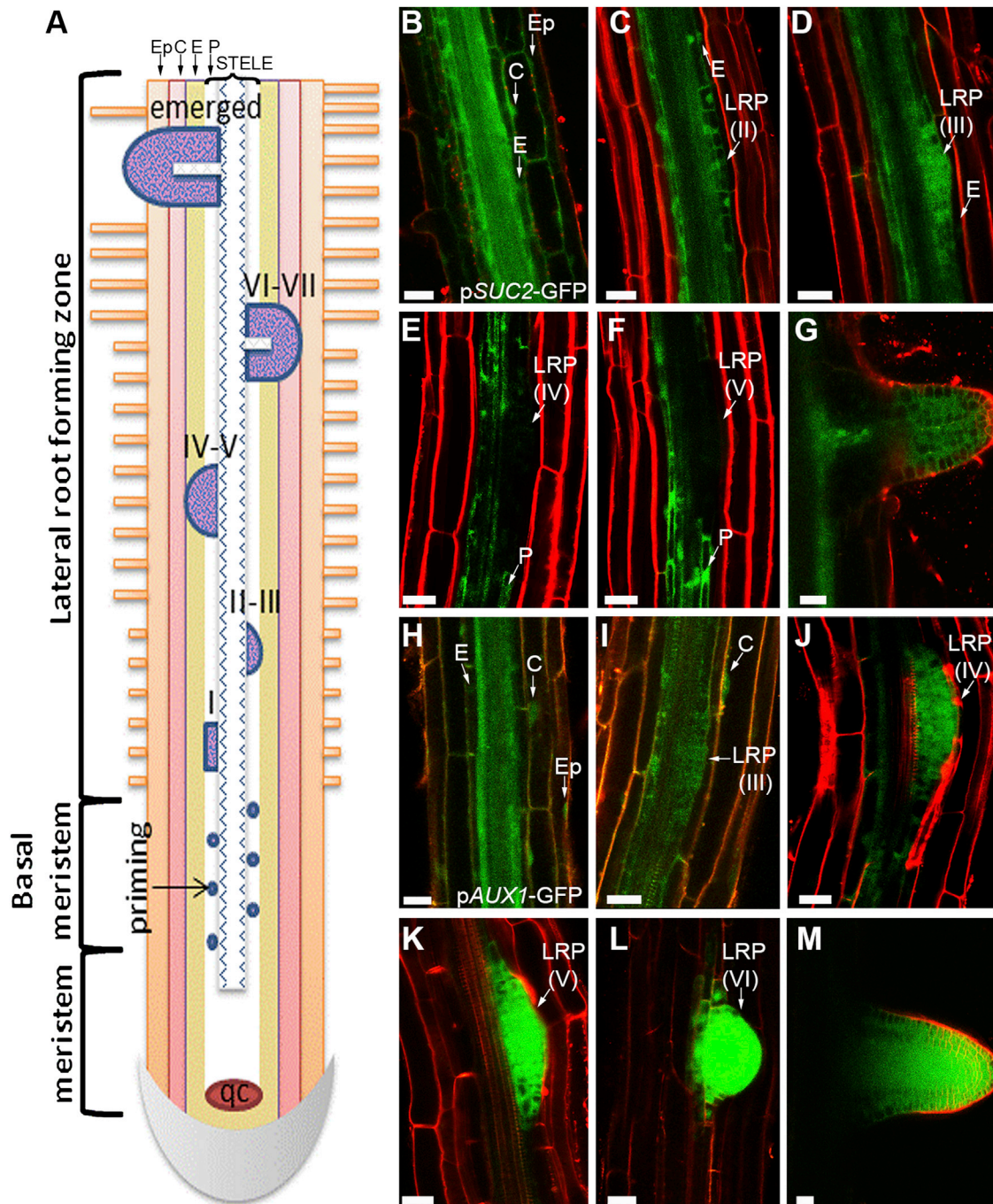


**Figure 1. Symplastic Domains Form during Lateral Root Development**

(A) Cartoon showing root developmental regions, LR stages, and tissue organization (qc, quiescent center; Ep, epidermis; C, cortex; E, endodermis; P, pericycle) as referred to in the text.

(B–M) Free GFP expression in pSUC2-GFP (B–G) and pAUX1-GFP (H–M) transgenic roots (10-day-old). Movement of GFP from the phloem (pSUC2-GFP) and from the pericycle (pAUX1-GFP) is observed into endodermal (E), cortical (C), and epidermal (Ep) cell layers in (B) and (H). GFP diffusion is gradually restricted as primordia develop (C–F, I–L; position of LRP and approximate stage in brackets are indicated). GFP unloading is normal in emerged lateral roots (G and M). FM4-64 (red) was used as counterstain. Stages were assigned according to bright-field images. Scale bars represent 20  $\mu$ m.

See also Figure S1.

i.e., total callose deposited around lateral roots increased progressively during development reaching a maximum in stage IV–V primordia (Figure S2F).

In summary, changes in symplastic transport during LR development correlate with changes in callose deposited suggesting a role for callose turnover in regulating symplastic connectivity in LRP.

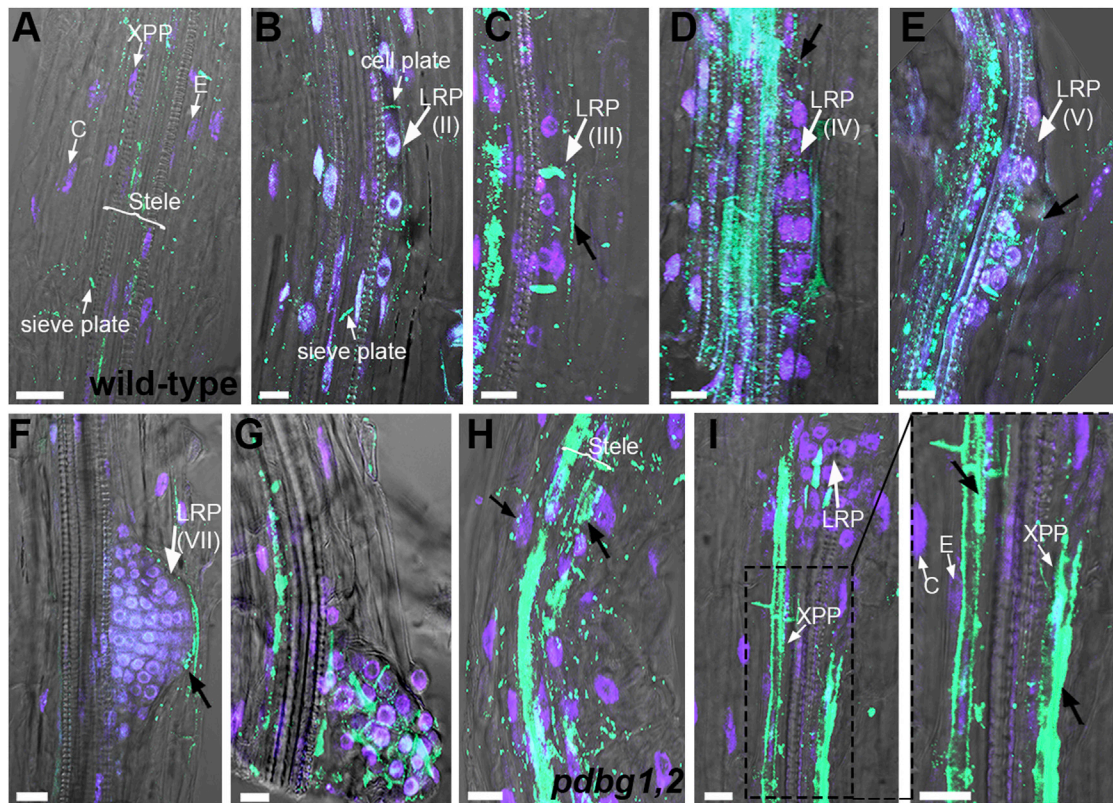


**Figure 2. Callose Deposition Is Regulated during Lateral Root Development and Is Increased in *pdbg1,2***

Immunofluorescent detection of callose (green) in the basal meristem (A), stage I–II (B), stage III (C), stage IV–V (D and E), stage VII (F), and emerged (G) primordia. Immunolocalization of callose in nonlateral root (H) and lateral root (I and inset) regions of *pdbg1,2* seedlings. Nuclei were stained with DAPI (blue) and bright-field images were superimposed. Black arrows indicate PD-associated callose. Cell plate- or sieve plate-associated callose, primordium (LRP), cortex (C), endodermis (E), XPP, and stele are also marked in (A), (B), and (I). Note the increase in callose deposited in the stele of *pdbg1,2* (H, I, and inset) in comparison to equivalent regions in wild-type (A and F). Scale bars represent 10  $\mu\text{m}$ .

See also Figures S2 and S4.

### Identification of Callose-Degrading Enzymes Associated with Lateral Roots and PDs

To identify proteins involved in the metabolism of PD-associated callose during LR organogenesis, we examined PD proteomic data. Thirteen putative callose metabolic enzymes (1,3- $\beta$ -D-glucanases and glucan synthases like [GSL]) were represented in published PD proteomes (Bayer et al., 2006; Fernandez-Calvino et al., 2011). We used transcriptome data sets (compiled in the VisualRTC) (Parizot et al., 2010) to screen for genes involved in lateral root initiation (Table S1). This approach identified At3g13560 as a putative  $\beta$ -1,3-glucanase preferentially expressed in the XPP (LR founder tissue) and that is induced by auxins in a SOLITARYROOT/IAA14-dependent manner. To confirm the expression of this gene in LR, we analyzed transgenic plants expressing the  $\beta$ -glucuronidase gene (GUS) downstream of the native promoter (Figure 3). At3g13560 (subsequently named *plasmodesmal-localized  $\beta$ -1,3-glucanase 1* [*PdBG1*]) is expressed at very low levels in the provasculature and vasculature of the basal meristem (Figures 3A and 3B). Interestingly, *PdBG1* was induced in few pericycle cells associated with the xylem in the early LR forming zone that might correspond

to sites of incipient primordia (Figure 3C). Expression increased soon after LR specification reaching a maximum at stage III primordia (Figures 3D–3F). This expression pattern was confirmed using a gene-trap insertion line that carries GUS fused to the N-terminal portion of the protein (Figures S3A–S3E).

To assess the cellular localization of *PdBG1*, we stably expressed an m-Citrine internal fusion (see Supplemental Experimental Procedures) in *Arabidopsis*. In leaves and roots, *PdBG1*-mCitrine accumulated in punctate spots at the cell periphery reminiscent of PD localization (Figures 3G and 3L). Confirming PD targeting, these spots colocalized with aniline blue stained-callose and with mCherry-PDCB1 (a plasmodesmal callose binding protein shown to associate with PD) (Simpson et al., 2009) (Figures 3H, 3I, 3M, and 3N). Supporting potential *PdBG1* activity in callose degradation, wound-induced callose was reduced in leaves overexpressing *PdBG1* (*PdBG1OE*) relative to wild-type (Figures 3O and 3P).

$\beta$ -1,3-glucanases are encoded by a large gene family (Doxey et al., 2007). Phylogenetic analysis and expression profile data identified a close evolutionary relationship between *PdBG1* and the genes At2g01630 (named *PdBG2*) and At1g66250

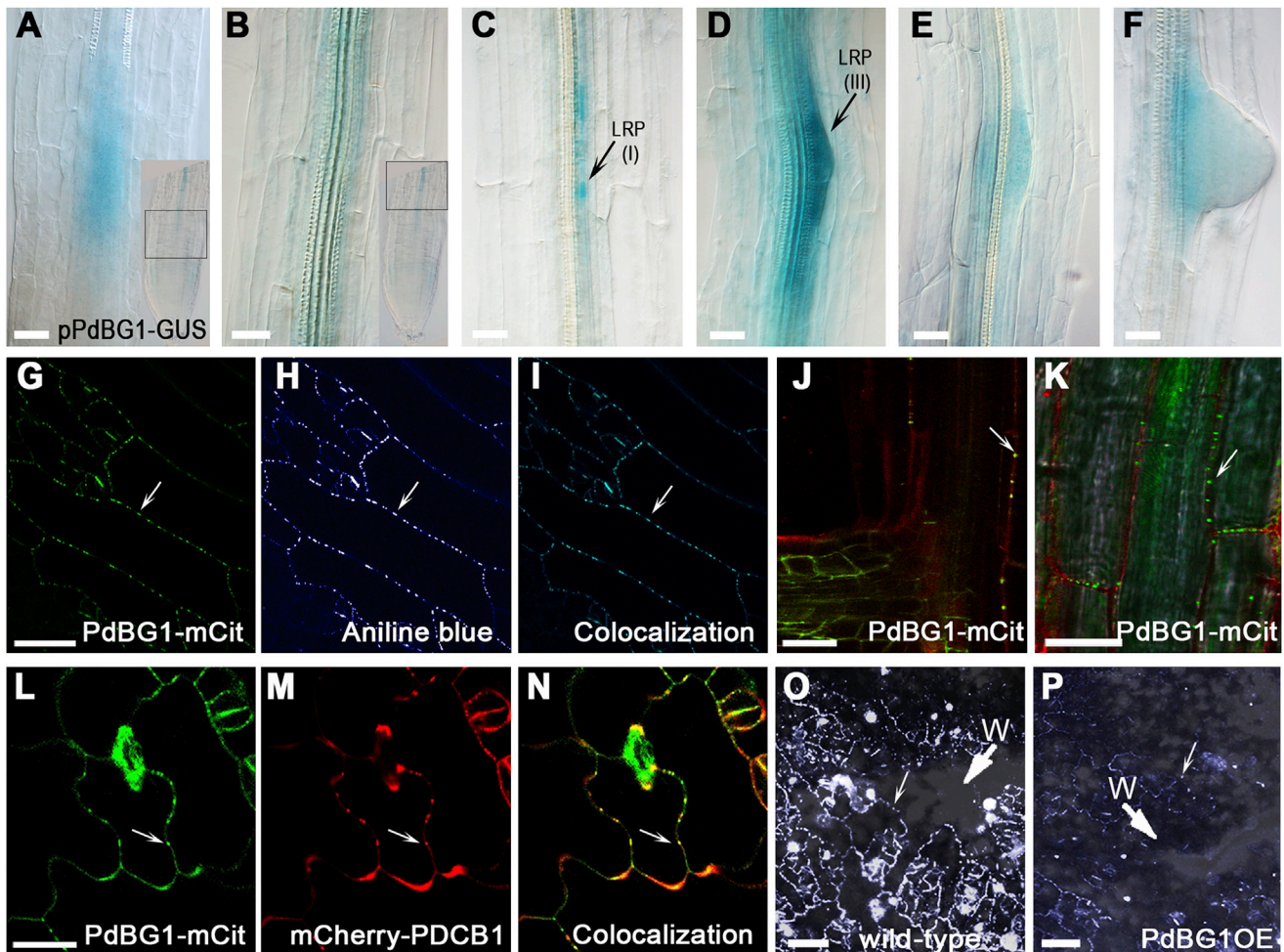


**Figure 3. PdBG1 Is a Callose-Degrading Enzyme Expressed in PDs of Early Stage Lateral Root Primordia**

(A–F) *PdBG1* expression as revealed by GUS staining of transgenics expressing *pPdBG1-GUS*. Expression is higher in potential lateral root founder cells and stage III LRP (black arrows). Small insets in (A) and (B) indicate the region imaged (square) using as reference the root tip (see also Table S1).

(G–I) *PdBG1-mCit* (mCitrine is fused in frame to the structural protein at position 452, green, G) and callose deposits revealed by aniline blue staining (false colored in white in H) colocalize at PD (I).

(J–P) As in leaves, *PdBG1-mCit* accumulates in a punctate pattern in the cell periphery of roots (J and K; FM4-64 stained cell periphery in red). *PdBG1-mCit* (L) also colocalizes with mCherry-PDCB1 (M) at PDs in transgenic leaves (N). Wound-induced callose (W indicates initial wounding site) is reduced in *PdBG1OE* (P) in comparison to wild-type (O). Scale bars represent 20  $\mu$ m.

See also Figure S3 and Table S1.

(named *PdBG3*). *PdBG2* and *PdBG3* m-Citrine-tagged constructs also showed PD localization, suggesting that they all act to control callose deposition at PD (Figures S3G–S3L). Moreover, microarray data indicate that *PdBG2* expression is high in XPP cells suggesting it might be involved in lateral root initiation (Table S1). To study *PdBG2* expression in lateral roots, we examined a line carrying a gene trap insertion in the first exon. *PdBG2* was upregulated in the stele, the LRP and, sporadically, in the endodermis associated with putative lateral root-founder cells (Figures S3M–S3R). This expression pattern partially overlaps with *PdBG1* suggesting that they might be functionally redundant genes.

The data identify two related callose degrading enzymes (*PdBG1* and *PdBG2*) that localize at PDs with expression patterns that implicate them in LR initiation and development.

### **PdBG1 and PdBG2 Regulate Callose Deposition and Symplastic Connectivity during Lateral Root Development**

To determine if *PdBG1* and *PdBG2* are involved in callose turnover during LR development, we examined callose deposition in *pdbg1*, *pdbg2*, and *pdbg1,2* double mutants. No significant difference was detected between single mutants and wild-type siblings, but the double mutant displayed a visible increase in fluorescence in the stele and lateral root primordia upon aniline blue staining (Figures S4A–S4D). Similar results were obtained using immunoassays: callose antibodies labeled more strongly *pdbg1,2* roots in comparison to wild-type siblings (Figures 2H and 2I). The differences were more pronounced in the stele of the basal meristem (Figure 2H) and pericycle associated with LRP (Figure 2I). Relative quantification of the increment in

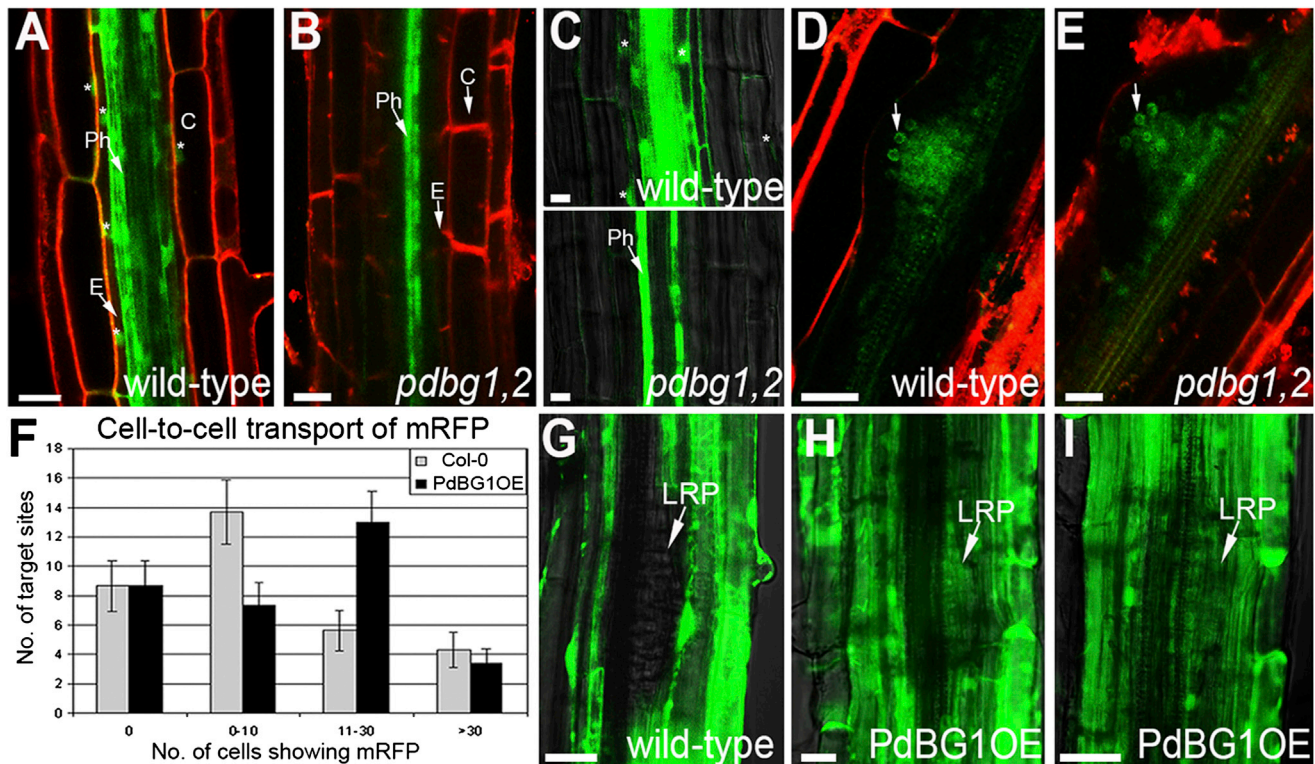


**Figure 4. Symplastic Transport Is Regulated by PdBG1 and PdBG2**

(A–C) GFP accumulation in the early LR forming zone (before any visible primordia) in *pdbg1,2* and wild-type siblings expressing *pSUC2*-GFP. GFP, primarily expressed in the phloem (Ph), moves (\*) to the endodermis (E) and cortex (C) in wild-type roots (A and C). Symplastic movement is blocked in *pdbg1,2* roots (B and C, lower panel).

(D and E) SHR-GFP expression and mobility (arrow) in wild-type and *pdbg1,2* lateral roots. FM4-64 (red) was used as a counterstain.

(F) Biolistic experiments using mRFP as symplastic probe. Data were collected in three experimental replicas for a total of 97 bombardment sites per genotype. The graph represents the number of sites that showed movement away from the bombardment target cell to 0 cells, 0–10 cells, 11–30 cells, and >30 cells. Error bars represent SEM.  $p < 0.001$  calculated by Poisson regression of the data.

(G–I) Dye transport after exposure of wild-type (G) and PdBG1OE (H and I) roots to CFDA. Notice dye loading into PdBG1OE primordia (H and I). Scale bars represent 20  $\mu$ m.

See also differences in callose deposition in Figure S4.

fluorescence signal indicated that *pdbg1,2* accumulated approximately three times more callose than wild-type roots (Figure S4F). In comparison, aniline blue fluorescence was significantly reduced in PdBG1OE (~2-fold decrease), supporting protein activity in callose degradation (Figures S4E and S4F).

Excessive callose deposition has been found to obstruct PDs blocking symplastic intercellular transport (Guseman et al., 2010; Vatén et al., 2011). To test symplastic transport in *pdbg1,2*, we studied GFP diffusion in mutants expressing *pSUC2*-GFP. In the basal meristem and early LR forming zone, GFP expressed in the phloem of wild-type siblings was able to move symplastically into the endodermis and cortex (Figures 1B, 4A, and 4C). Conversely, in *pdbg1,2* roots, GFP was retained in the phloem (Figures 4B and 4C). This was consistent with the increase in stele-associated callose observed in *pdbg1,2* root (Figure 2H). Excessive callose deposition has been shown to affect the transport of the SHORTROOT protein (SHR) from the stele to the endodermis (Vatén et al., 2011). In *pdbg1,2* mutants transformed with *pSHR::SHR*-GFP, we could not detect changes in SHR-GFP transport relative to siblings in the wild-

type background (Figures 4D and 4E) consistent with the low level of expression detected for *PdBG1* and *PdBG2* in emerging LRP (Figures 3E and 3F).

Because the double mutant displayed a reduction in symplastic connectivity, overexpression will likely have the reverse effect. Supporting this hypothesis, we showed that mRFP, produced from bombarded mRFP cDNA, more frequently moved further (number of cells showing mRFP) in PdBG1OE leaves in comparison to wild-type (Figure 4F). Moreover, symplastic diffusion of CFDA (carboxyfluorescein diacetate) in roots exposed for 5 min to the dye, was enhanced in PdBG1OE stage IV–VI primordia in comparison to wild-type (Figures 4G–I).

Together these results indicate that PdBGs are necessary and sufficient to regulate callose and intercellular transport during development of lateral root primordia.

#### Changes in Callose Accumulation and PD Flux Affect Lateral Root Initiation and Distribution

The localization and pattern of expression for the PdBG proteins suggest that they might play a role in lateral root development.

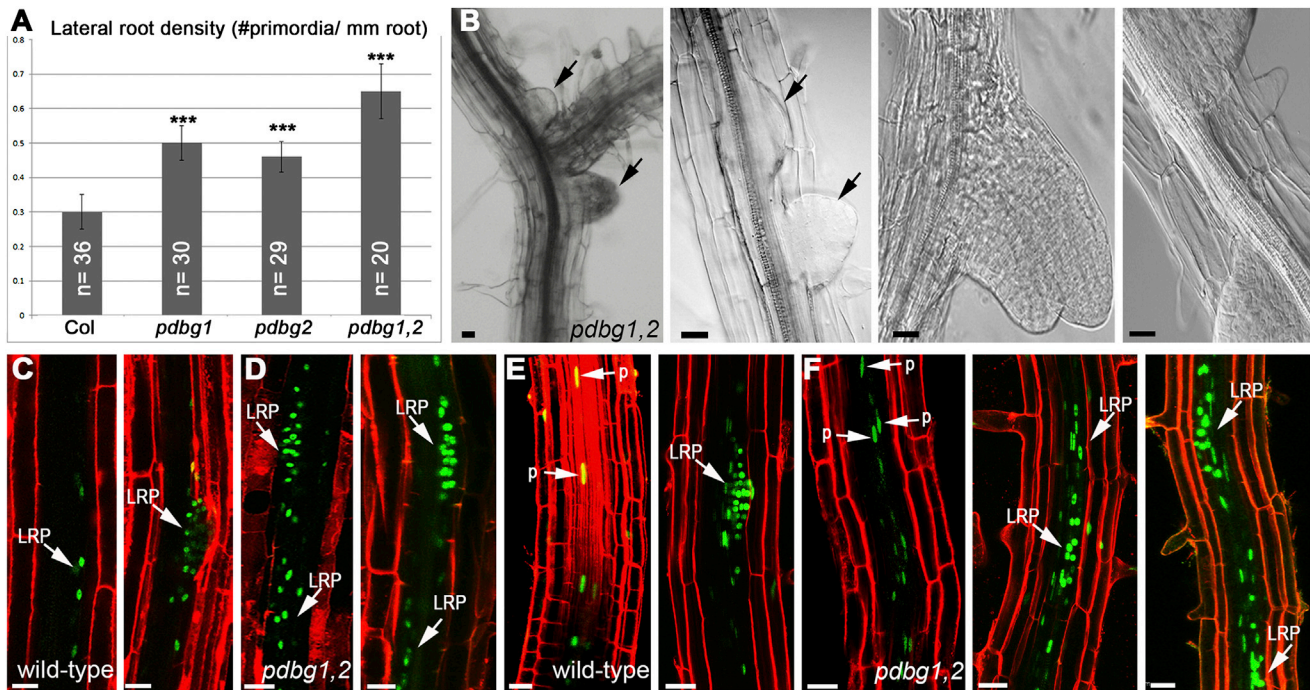


**Figure 5. Mutations in PdBG1 and PdBG2 Affect Lateral Root Density by Altering the Spacing between Primordia**

(A) Lateral root density was calculated for 6-day-old Col-0, *pdbg1*, *pdbg2*, and *pdbg1,2* roots. Error bars represent SD (\*\**p* < 0.001).

(B) Examples of clustered and fused lateral roots found in *pdbg1,2*.

(C–F) In comparison to wild-type siblings (C), *pdbg1,2* showed extended regions of *GATA23* (D) expression. Similarly, spacing between maxima of *DR5* expression in the priming region (p, prebranch sites) and in the lateral root forming zone of wild-type siblings (E) is not maintained in the mutant (F). These results are consistent with the formation of clustered primordia (LRP). Roots were stained with FM4-64 (red). Scale bars represent 20  $\mu$ m.

See also Figure S5.

To further investigate this hypothesis, we studied the lateral root phenotype of PdBG mutants and overexpression lines. Lateral root density (number of LR initiation events per mm of root) has been used to characterize defects in LR development (Benková and Bielach, 2010). *pdbg1*, *pdbg2*, and double mutants, in both Col-0 and Ler backgrounds, showed an increase in the number of initiated primordia relative to wild-type roots (Figures 5A and S5A). The effect was stronger in *pdbg1,2* double mutant roots, confirming that these genes have partially redundant functions.

Closer examination of mutant roots showed that primordia frequently formed adjacent to each other that occasionally led to the emergence of a fused LR (Figure 5B). To investigate this phenotype, we created transgenic plants expressing a reporter for *GATA23*, a gene that controls LR-founder cell specification (De Rybel et al., 2010). In wild-type roots, *GATA23* peaks of expression were regularly spaced that was coincident with the normal distribution of LRP along the main root (Figures 5C and 6B). In contrast, *pdbg1,2* had extended domains of *GATA23* expression that correlated with the initiation of LR in clusters (Figure 5D).

It has been reported that the relative position and distance between lateral roots are marked by periodic pulses of *DR5* expression in the oscillatory zone (prebranch sites) (Moreno-Risueno et al., 2010). Because *pdbg1,2* displayed altered callose deposition and symplastic transport in the basal meristem

(which contains the oscillatory zone) and formed fused primordia, we investigated LR priming by expressing the reporter *pDR5-3xVENUS-N7* (Brunoud et al., 2012) in wild-type and *pdbg1,2* roots. Although the reporter was induced at regular intervals in the oscillatory zone of wild-type roots (Figure 5E), priming sites seem clustered together in the mutant (Figure 5F). *DR5* expression overlapped with *GATA23* in LRP and, as before, extended domains of *DR5* expression in *pdbg1,2* indicated disrupted primordia spatial patterning (compare panels in Figures 5E and 5F).

Consistent with a role for PdBG in lateral root initiation, PdBG1OE showed the reciprocal effect: a significant decrease in lateral root density (Figure 6A). In agreement with this observation, the distance between *GATA23*-marked initiation sites was larger in PdBG1OE when compared with wild-type siblings suggesting that primordia are spread more widely in this line (Figures 6B, 6C, and 6F).

Defects in lateral root initiation are often correlated with impaired maintenance of the apical meristem and/or altered emergence because these processes share some commonalities in their signaling pathways (Aloni et al., 2006; Lucas et al., 2008; Péret et al., 2009). To investigate the role of PdBGs in root meristem development and LR emergence, we quantified root meristem size and percentage of emergence in *pdbg1,2* and PdBG1OE lines. Although double mutant and overexpressors had opposite effect on callose and lateral root number,

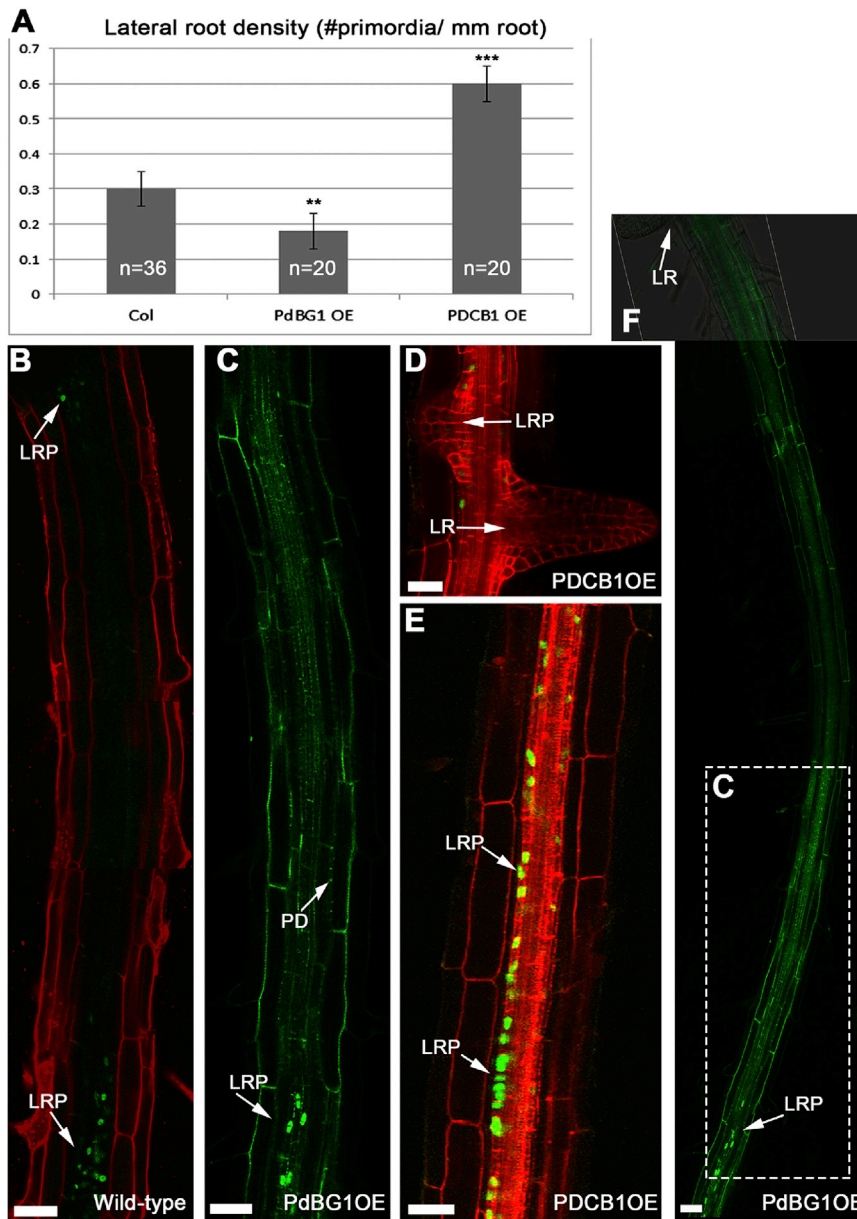


**Figure 6. Callose Deposition Regulates the Spacing between Lateral Root Initiation Sites**

(A) Lateral root density in PdBG1OE and PDCB1OE roots (\*\*p < 0.01; \*\*\*p < 0.001). Error bars represent SD.

(B–E) *GATA23* expression (green nuclei) in wild-type (B), PdBG1OE (C), and in PDCB1OE roots (D and E). In comparison to wild-type (B), overexpression of PdBG1 led to a significant increase in the distance between primordia (C). Conversely, primordia appear clustered in PDCB1OE (D and E). (F) The same root represented in (C) at smaller scale to appreciate the distance between the LRP and the nearest LR (arrowed). Wild-type roots were stained with FM4-64 (red) in (B). Cell-walls fluoresce in green in (C) and (F) due to PdBG1-mCit expression at PD and in red in (D) and (E) due to mCherry-PDCB1. Scale bars represent 40  $\mu$ m (B, C, and F) and 20  $\mu$ m (D and E).

See also emergence phenotype in Figure S6.

these developmental processes, we synchronized primordia initiation by applying a gravitropic stimulus to 3-day-old roots. Primordia initiate synchronously 12 hr after root bending and fully emerge 48 hr postgravitimulation (Péret et al., 2012). We could not detect differences in the percentage of “emerging” primordia 42 hr postgravitimulation between either *pdbg1,2* or PdBG1OE and wild-type roots suggesting that emergence is not directly regulated by these genes (Figures S6B and S6C).

The phenotypes described in mutant and overexpression lines suggest that PdBG1,2 are primarily involved in LR initiation and spatial patterning. To address if PdBG activity on callose degradation is directly responsible for these phenotypic defects, we examined LR density in a PDCB1 overexpression line. Ectopic expression of PDCB1 has been shown to decrease symplastic transport and

they both showed a mild reduction in meristem size in comparison to wild-type and were similar in appearance at the whole plant scale (Figures S5B and S5C). This suggests that these genes are not main regulators of apical meristem development. Supporting this conclusion, callose was deposited at similar levels in wild-type and *pdbg1,2* apical root meristem regions (Figures S5D and S5E).

To complement our observations, we examined the percentage of LR emergence in mutant and overexpressing lines. The percentage of emerged LR was similar in *pdbg1*, *pdbg2* single and double mutants and wild-type but increased in PdBG1OE (Figure S6A). Increased emergence in PdBG1OE could be directly caused by ectopic expression of this cell wall modifying enzyme (Swarup et al., 2008) or an indirect consequence of the reduction in primordia initiation (Lucas et al., 2008). To uncouple

increase callose deposition at PD neck regions (Simpson et al., 2009). We found that similar to *pdbg1,2*, PDCB1OE showed increased LR density (Figure 6A) and neighboring primordia that corresponded with clustered sites of *GATA23* expression (Figures 6D and 6E). This result provides independent evidence that links callose to the regulation of lateral root patterning.

To further demonstrate the importance of callose regulation in this process, we studied inducible transgenic lines expressing a mutated/activated version of PD-located CALS3 (*cals3m*). Induction of *cals3m* has been shown to modify PD-associated callose and symplastic transport within 48 hr (Vatén et al., 2011). To express this protein specifically in the XPP (LR competent tissue), we transformed an estradiol-inducible UAS promoter driving *cals3m* into the enhancer-trap line J0121 (Figure 7A) (Parizot et al., 2008). This construct was named

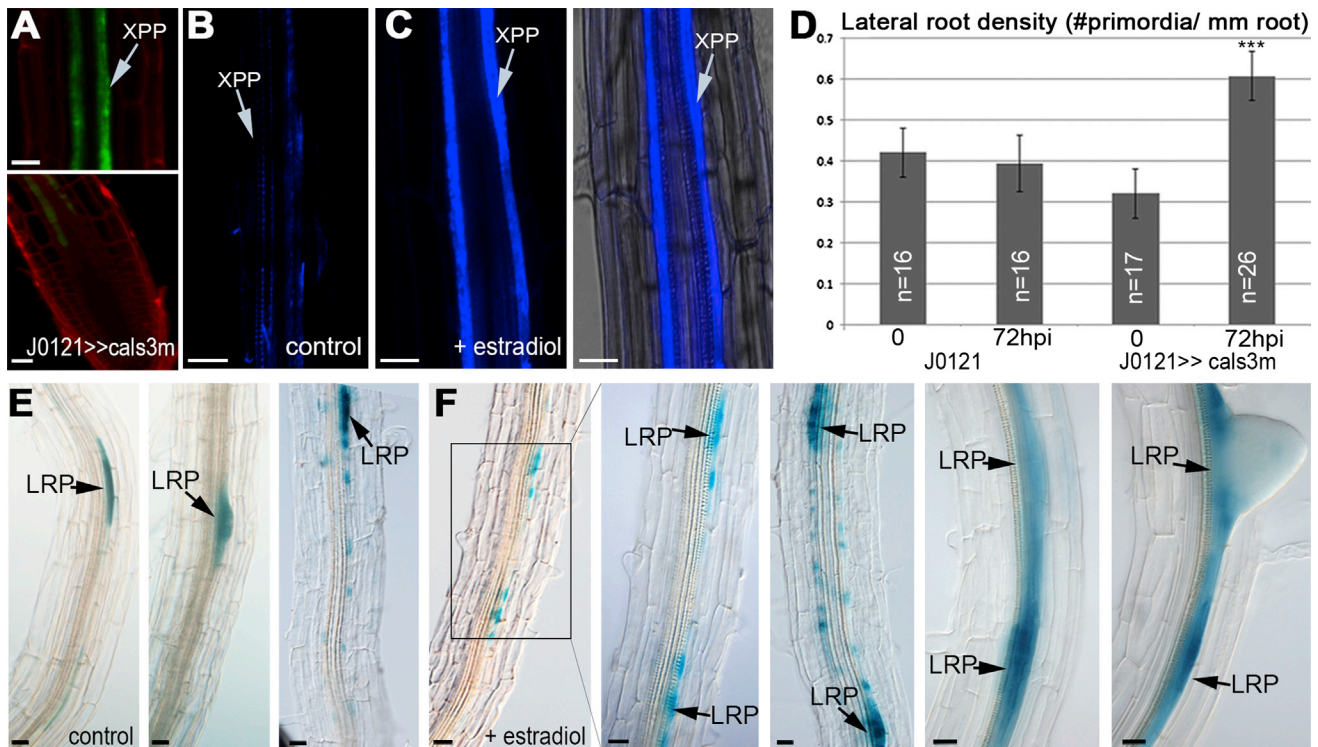


**Figure 7. Altered Lateral Root Distribution Is a Primary Effect of Induced Callose Deposition in the Xylem-Pole Pericycle**

(A–C) Pattern of GFP expression in root tissues of the GAL4–GFP enhancer trap line J0121 is associated with mature XPP. Aniline blue staining revealed increased callose deposition after 24 hr estradiol treatment of roots expressing *cals3m* under an estradiol-inducible UAS promoter in the J0121 background (J0121>>*cals3m*) in comparison to noninduced control siblings (B and C). Bright-field superimposed image is also shown for (C).

(D) Lateral root density in control (J0121 and untreated J0121>>*cals3m*) and estradiol-treated roots calculated 72 hr postinduction (hpi). Error bars represent SD (\*\**p* < 0.001). LR primordia (arrows) are marked by GUS activity in control (E, panels) and induced (48 hpi) J0121>>*cals3m* (F, panels) transgenics expressing pGATA23–GUS. Notice the neighboring primordia in (F) panels. Scale bars represent 20  $\mu$ m.

J0121>>*cals3m*. In our conditions, 24 hr of estradiol treatment was sufficient to produce a significant amount of callose in the XPP (Figures 7B and 7C). Lateral root density was analyzed in estradiol-treated and mock-treated lines 72 hr postinduction (48 hr after increase callose deposition was confirmed). As expected, the number of initiated primordia was significantly higher in induced J0121>>*cals3m*, consistent with a role for PD-associated callose in lateral root initiation (Figure 7D). We used the *GATA23* promoter to drive GUS expression in the callose inducible lines to monitor LR initiation. Forty-eight hours estradiol induction of J0121>>*cals3m* induced the initiation of neighboring LRP and clusters reported by large domains of *GATA23* expression (Figures 7E and 7F). This result confirms that callose regulation of intercellular connectivity between pericycle cells, founder cells, and the neighboring tissue is important to establish lateral root patterning in *Arabidopsis*.

## DISCUSSION

Lateral root formation has been attributed to auxin gradients that trigger initiation events in the root pericycle. This causes redifferentiation of lateral root founder cells and the formation of new meristems. Mobile signals (including, but not restricted to auxins) have been proposed to play a role in the relative positioning of primordia and the emergence phase of lateral root development

(De Smet et al., 2008; Péret et al., 2012; Moreno-Risueno et al., 2010; Van Norman et al., 2011; Marin et al., 2010; Meng et al., 2012). We have identified that symplastic domains are regulated around LRP, through a mechanism that involves the deposition of PD-associated callose. This process regulates intercellular signaling and is fundamental to the definition of LR spatial patterning.

Our data indicate that prior to and during LRP specification all cells are symplastically connected to the pericycle. Hence GFP diffuses readily through the cells of the stele and outer tissues (Figure 1). Following the first pericycle cell divisions, symplastic connectivity is reduced, which correlates with an increase in callose deposited around stage IV–V primordia. In agreement with our results, previous studies using dye loading experiments reported that symplastic continuity between the emerging primordia and the phloem of the primary root is lost and only reestablished when a new phloem connection is formed (Oparka et al., 1995). The reasons behind this late downregulation in symplastic transport might lie in the need to maintain water pressure (and tissue hydraulics) relevant during the emergence phase (Péret et al., 2012), but questions remain regarding the role of symplastic regulation early in LRP development.

PdBG1 and PdBG2 are PD-located callose degrading enzymes expressed in the stele and early stages primordia. PdBG1 and PdBG2 are induced in auxin-treated roots but not

in the mutant *solitary root1*, suggesting that they are potential targets of the auxin signaling pathway that regulates lateral root initiation (Vanneste et al., 2005). Interestingly, PdBG orthologs in *Populus* are upregulated during dormancy release suggesting a role for these enzymes in shoot meristem development (Rinne et al., 2011).

We demonstrated that symplastic connectivity in the basal meristem and lateral root-forming zone depend on PdBG1/PdBG2 activity. Moreover, these enzymes influence LR initiation and positioning. Double mutants *pdbg1,2* are impaired in callose degradation and exhibit restricted PD transport, higher LR density, and distorted primordia patterning (Figures 2, 4, and 5). LR phenotypes caused by the absence of PdBG1 and/or PdBG2 are associated with the function of these proteins during LR initiation and not emergence (Figure S6). As expected, overexpression of PdBG1 produced the opposite effect with respect to LR density and patterning. Interestingly, the auxin-response factor DR5 is induced in neighboring pericycle cells in the basal meristem of *pdbg1,2* that implicates symplastic connectivity in the establishment of prebranching sites. Temporal and spatial distribution of LRs is established by the oscillating expression of genes that determine periodic root branching and bending (Moreno-Risueno et al., 2010). Cell-to-cell connectivity might regulate the mobility of factors that originate in primed cells to repress lateral root initiation in adjacent pericycle cells or the transport of a LR inhibitory signal from neighboring tissues into the XPP (Traas and Vernoux, 2010). Both models predict an increase in the number of lateral root initiated when reducing symplastic communication in the XPP. Supporting this hypothesis, increasing callose deposition by expressing ectopically PDCB1 or CALS3 in the XPP (in estradiol-treated J0121>>cals3m) increased LR density and reduced the spacing between initiated primordia (Figures 6 and 7).

We propose that regulated intercellular connectivity plays a central role in LR development specifically by influencing the number and spatial organization of pericycle cells forming lateral roots. This adds a facet to our understanding of LR organogenesis and patterning beyond the well-studied role of hormones. In identifying that regulation of symplastic connectivity, by callose turnover, is essential to LR patterning these data raise intriguing questions relating to the nature of crosstalk between hormone signaling and symplastic communication. PD connectivity might regulate the non-cell-autonomous activity of auxin-inducible factors, such as Target of MONOPTEROS 7 (Schlereth et al., 2010). Interestingly, a role for MONOPTEROS/ARF5-dependent pathways in the control of cell division and identity in the pericycle has previously been described (De Smet et al., 2010). Future work will address the intricacies of these mechanisms that are fundamental to the establishment of optimal root architecture and for general plant performance.

## EXPERIMENTAL PROCEDURES

### Plant Material

*Arabidopsis thaliana* Columbia (Col-0) knockout lines were obtained for PdBG1 (SAIL\_389\_H11), PdBG2 (SALK\_046127), and PdBG3 (SALK\_14587) from the Nottingham Arabidopsis Stock Centre. We also obtained transposon insertional mutants (insertions in the same orientation of the gene) in Ler background from the Cold Spring Harbor Laboratory (<http://genetrap.cshl.edu>) and John Innes Centre SM lines collection for PdBG1 (GT\_5\_41639),

PdBG2 (GT10161), and PdBG3 (ET82). The *pdbg1,2* double mutant, in Col and Ler background, was generated by crossing the single mutant lines. Primers for genotyping are in the Supplemental Experimental Procedures.

Seeds were sterilized and germinated in long day conditions on plates containing MS medium. For estradiol induction, seedlings were germinated in MSO (MS without sucrose) and transferred after 6 days to MSO supplemented with 10  $\mu$ M 17  $\beta$ -estradiol. Lateral root phenotypes were evaluated at 24 hr, 48 hr, and 72 hr after treatment.

### Generation of Transgenics

Transgenic seeds expressing pGATA23::GUS-nlsGFP, pSHR::SHR:GFP, pSUC2::mGFP6, pAUX1::AUX1:YFP, and pDR5::3xVENUS were requested (De Rybel et al., 2010; Brunoud et al., 2012; Benitez-Alfonso et al., 2009; Nakajima et al., 2001; Swarup et al., 2004). Construction of the p35S::mCherry-PDCB1 (PDCB1OE) has been described before (Simpson et al., 2009). In all cases, expression of the constructs in mutant or overexpression background was achieved by crossing transgenic lines.

The inducible line J0121>>icals3m was obtained by introducing the p6xUAS::icals3m expressed in a modified version of pER8 (an estrogen-receptor-based chemical-inducible system) in the enhancer trap line J0121 (<http://www.plantsci.cam.ac.uk/Haseloff/>) as described elsewhere (Vatén et al., 2011).

The syntheses of pAUX1-GFP as well as m-Citrine tagged constructs for PdBG1 (At3g13560, accession number NM\_202574), PdBG2 (At2g01630, accession number NM\_126224.2), and PdBG3 (At1g66250, accession number NM\_105296.2) are described in the Supplemental Experimental Procedures. Construction of pPdBG1-GUS and pPdBG1-PdBG1-mCit are also described.

### GUS Staining and Dye Loading

Standard protocols were used for GUS assays (Simpson et al., 2009). Stained roots were mounted in chloral hydrate solution (1.3 g/ml chloral hydrate, 33% glycerol) and visualized in a Leica DM 6000.

To assess symplastic permeability, 10-day-old roots were exposed to 50  $\mu$ g/ml carboxyfluorescein diacetate (CFDA, Sigma) for 5 min and 30 min and thoroughly washed with water before microscopy. Differences in dye loading between PdBG1OE and wild-type were evident after 5 min staining.

### Callose Staining, Immunolocalization, and Quantification

Protocols for callose detection using immunolocalization or aniline blue staining are provided in the Supplemental Experimental Procedures.

To analyze wound-induced callose, leaves were pierced with tweezers and immediately infiltrated with aniline blue solution. For quantification, confocal images of aniline blue-stained roots were taken at the same resolution (pinhole) avoiding over-exposure. Regions of interest (ROI) were drawn in comparable developmental areas containing LRP and/or immediately adjacent tissue and the mean gray value was determined using LAS AS Lite Software. At least three independent replicates were used to calculate each average and SD using M. Excel package.

### Microscopy

For counterstaining, roots were briefly exposed to 0.1  $\mu$ g/ml FM4-64 (Invitrogen) before microscopy. Confocal analysis was performed on a Leica SP5 or Zeiss LSM510 confocal microscopes using a 488 nm excitation laser for GFP, m-Citrine, and Alexa 488, the 405 nm laser for aniline blue fluorochrome and DAPI, and 561 nm (DPSS) laser for mRFP and mCherry.

For anatomical, histological, and reporter gene analyses, 10-day-old roots from vertically grown seedlings were used. Images were captured digitally with a Leica DM6000 equipped with Nomarski optics (DIC) and analyzed with the ImageJ software (<http://rsbweb.nih.gov/ij/>).

### Microprojectile Bombardment

Microprojectile bombardment assays were performed as described (Thomas et al., 2008). Expanded 4- to 6-week-old leaves of relevant *Arabidopsis* lines were bombarded with gold particles coated with pB7WG2.0.mRFP using a Bio-Rad Biolistic PDS-1000/He Particle Delivery System. Bombardment sites were imaged 24 hr postbombardment by confocal microscopy. Data were collected for a total of 97 bombardment sites for each genotype from at least three independent bombardment experiments, each of which consisted of

leaves from at least two individual plants. Statistical Poisson regression analysis was performed using GraphPad Prism version 5.04.

#### Statistical Analysis of Meristem Size, Lateral Root Density, and Emergence Phenotypes

Cleared root preparations were characterized as described (Dubrovsky and Forde, 2012). We recorded the total number of primordia and emerged lateral roots (new meristems sticking out the main root) as well as total root length in 10-day-old seedlings to calculate density (number of lateral root initiation events per mm of main root) and emergence (percentage of emerged lateral roots from the total number of lateral root initiation events). To investigate emergence phenotypes, we synchronized lateral root initiation by applying a gravitropic stimulus (90° rotation of plates) to 3-day-old seedlings grown vertically on 0.5× MS plates (Péret et al., 2012) and counted the number of emerging (stage VII) primordia, in the outer edge of the bend, 42 hr after gravistimulation. We measured root meristem size as the distance from the QC to the end of cell division. *p* value was calculated using two-tailed Student's *t* test.

#### SUPPLEMENTAL INFORMATION

Supplemental Information includes Supplemental Experimental Procedures, six figures, and one table and can be found with this article online at <http://dx.doi.org/10.1016/j.devcel.2013.06.010>.

#### ACKNOWLEDGMENTS

We thank T. Beeckman and M.J. Bennett for kindly providing the GATA23 and the DR5 reporter lines. SHR and AUX1 translational fusion lines were obtained from P. Benfey and C. Kuhlemeier, respectively. We acknowledge the contribution of C. Burt in statistical analysis and K.D. O'Neill and J. Barnes in technical support. The John Innes Centre is grant-aided by the Biotechnology and Biological Science Research. The authors want to acknowledge the retirement of A.M. from active research.

Received: September 19, 2012

Revised: April 5, 2013

Accepted: June 11, 2013

Published: July 11, 2013

#### REFERENCES

- Aloni, R., Aloni, E., Langhans, M., and Ullrich, C.I. (2006). Role of cytokinin and auxin in shaping root architecture: regulating vascular differentiation, lateral root initiation, root apical dominance and root gravitropism. *Ann. Bot. (Lond.)* 97, 883–893.
- Bayer, E.M., Bottrill, A.R., Walshaw, J., Vigouroux, M., Naldrett, M.J., Thomas, C.L., and Maule, A.J. (2006). Arabidopsis cell wall proteome defined using multidimensional protein identification technology. *Proteomics* 6, 301–311.
- Benitez-Alfonso, Y., Cilia, M., San Roman, A., Thomas, C., Maule, A., Hearn, S., and Jackson, D. (2009). Control of Arabidopsis meristem development by thioredoxin-dependent regulation of intercellular transport. *Proc. Natl. Acad. Sci. USA* 106, 3615–3620.
- Benitez-Alfonso, Y., Jackson, D., and Maule, A. (2011). Redox regulation of intercellular transport. *Protoplasma* 248, 131–140.
- Benková, E., and Bielach, A. (2010). Lateral root organogenesis—from cell to organ. *Curr. Opin. Plant Biol.* 13, 677–683.
- Brunoud, G., Wells, D.M., Oliva, M., Larrieu, A., Mirabet, V., Burrow, A.H., Beeckman, T., Kepinski, S., Traas, J., Bennett, M.J., and Vernoux, T. (2012). A novel sensor to map auxin response and distribution at high spatio-temporal resolution. *Nature* 482, 103–106.
- Chen, X.Y., Liu, L., Lee, E., Han, X., Rim, Y., Chu, H., Kim, S.W., Sack, F., and Kim, J.Y. (2009). The Arabidopsis callose synthase gene *GSL8* is required for cytokinesis and cell patterning. *Plant Physiol.* 150, 105–113.
- De Rybel, B., Vassileva, V., Parizot, B., Demeulenaere, M., Grunewald, W., Audenaert, D., Van Campenhout, J., Overvoorde, P., Jansen, L., Vanneste, S., et al. (2010). A novel aux/IAA28 signaling cascade activates GATA23-dependent specification of lateral root founder cell identity. *Curr. Biol.* 20, 1697–1706.
- De Smet, I., Vanneste, S., Inzé, D., and Beeckman, T. (2006). Lateral root initiation or the birth of a new meristem. *Plant Mol. Biol.* 60, 871–887.
- De Smet, I., Vassileva, V., De Rybel, B., Levesque, M.P., Grunewald, W., Van Damme, D., Van Noorden, G., Naudts, M., Van Isterdael, G., De Clercq, R., et al. (2008). Receptor-like kinase ACR4 restricts formative cell divisions in the Arabidopsis root. *Science* 322, 594–597.
- De Smet, I., Lau, S., Voss, U., Vanneste, S., Benjamins, R., Rademacher, E.H., Schlereth, A., De Rybel, B., Vassileva, V., Grunewald, W., et al. (2010). Bimodular auxin response controls organogenesis in Arabidopsis. *Proc. Natl. Acad. Sci. USA* 107, 2705–2710.
- Doxey, A.C., Yaish, M.W., Moffatt, B.A., Griffith, M., and McConkey, B.J. (2007). Functional divergence in the Arabidopsis beta-1,3-glucanase gene family inferred by phylogenetic reconstruction of expression states. *Mol. Biol. Evol.* 24, 1045–1055.
- Dubrovsky, J.G., and Forde, B.G. (2012). Quantitative analysis of lateral root development: pitfalls and how to avoid them. *Plant Cell* 24, 4–14.
- Fernandez-Calvino, L., Faulkner, C., Walshaw, J., Saalbach, G., Bayer, E., Benitez-Alfonso, Y., and Maule, A. (2011). Arabidopsis plasmodesmal proteome. *PLoS ONE* 6, e18880.
- Guseman, J.M., Lee, J.S., Bogenschutz, N.L., Peterson, K.M., Virata, R.E., Xie, B., Kanaoka, M.M., Hong, Z., and Torii, K.U. (2010). Dysregulation of cell-to-cell connectivity and stomatal patterning by loss-of-function mutation in Arabidopsis *chorus* (glucan synthase-like 8). *Development* 137, 1731–1741.
- Kim, J.Y., Yuan, Z., Cilia, M., Khalfan-Jagani, Z., and Jackson, D. (2002). Intercellular trafficking of a KNOTTED1 green fluorescent protein fusion in the leaf and shoot meristem of Arabidopsis. *Proc. Natl. Acad. Sci. USA* 99, 4103–4108.
- Kim, J.Y., Yuan, Z., and Jackson, D. (2003). Developmental regulation and significance of KNOX protein trafficking in Arabidopsis. *Development* 130, 4351–4362.
- Lee, J.Y., Wang, X., Cui, W., Sager, R., Modla, S., Czymmek, K., Zybaliov, B., van Wijk, K., Zhang, C., Lu, H., and Lakshmanan, V. (2011). A plasmodesmata-localized protein mediates crosstalk between cell-to-cell communication and innate immunity in Arabidopsis. *Plant Cell* 23, 3353–3373.
- Levy, A., Erlanger, M., Rosenthal, M., and Epel, B.L. (2007a). A plasmodesmata-associated beta-1,3-glucanase in Arabidopsis. *Plant J.* 49, 669–682.
- Levy, A., Guenoune-Gelbart, D., and Epel, B.L. (2007b). beta-1,3-Glucanases: plasmodesmal gate keepers for intercellular communication. *Plant Signal. Behav.* 2, 404–407.
- Lucas, M., Guédon, Y., Jay-Allemand, C., Godin, C., and Laplace, L. (2008). An auxin transport-based model of root branching in Arabidopsis thaliana. *PLoS ONE* 3, e3673.
- Malamy, J.E., and Benfey, P.N. (1997). Organization and cell differentiation in lateral roots of Arabidopsis thaliana. *Development* 124, 33–44.
- Marchant, A., Bhalerao, R., Casimiro, I., Eklöf, J., Casero, P.J., Bennett, M., and Sandberg, G. (2002). AUX1 promotes lateral root formation by facilitating indole-3-acetic acid distribution between sink and source tissues in the Arabidopsis seedling. *Plant Cell* 14, 589–597.
- Marin, E., Jouannet, V., Herz, A., Lokerse, A.S., Weijers, D., Vaucheret, H., Nussaume, L., Crespi, M.D., and Maizel, A. (2010). miR390, Arabidopsis TAS3 tasiRNAs, and their AUXIN RESPONSE FACTOR targets define an autoregulatory network quantitatively regulating lateral root growth. *Plant Cell* 22, 1104–1117.
- Meng, L., Buchanan, B.B., Feldman, L.J., and Luan, S. (2012). CLE-like (CLEL) peptides control the pattern of root growth and lateral root development in Arabidopsis. *Proc. Natl. Acad. Sci. USA* 109, 1760–1765.
- Moreira, S., Bishopp, A., Carvalho, H., and Campilho, A. (2013). AHP6 inhibits cytokinin signaling to regulate the orientation of pericycle cell division during lateral root initiation. *PLoS ONE* 8, e5370.

- Moreno-Risueno, M.A., Van Norman, J.M., Moreno, A., Zhang, J., Ahnert, S.E., and Benfey, P.N. (2010). Oscillating gene expression determines competence for periodic *Arabidopsis* root branching. *Science* 329, 1306–1311.
- Muraro, D., Byrne, H., King, J., and Bennett, M. (2013). The role of auxin and cytokinin signalling in specifying the root architecture of *Arabidopsis thaliana*. *J. Theor. Biol.* 317, 71–86.
- Nakajima, K., Sena, G., Nawy, T., and Benfey, P.N. (2001). Intercellular movement of the putative transcription factor SHR in root patterning. *Nature* 413, 307–311.
- Oparka, K.J., Prior, D., and Wright, K.M. (1995). Symplastic communication between primary and developing lateral roots of *Arabidopsis thaliana*. *J. Exp. Bot.* 46, 187–197.
- Parizot, B., Laplace, L., Ricaud, L., Boucheron-Dubuisson, E., Bayle, V., Bonke, M., De Smet, I., Poethig, S.R., Sr., Helariutta, Y., Haseloff, J., et al. (2008). Diarch symmetry of the vascular bundle in *Arabidopsis* root encompasses the pericycle and is reflected in distich lateral root initiation. *Plant Physiol.* 146, 140–148.
- Parizot, B., De Rybel, B., and Beeckman, T. (2010). VisualRTC: a new view on lateral root initiation by combining specific transcriptome data sets. *Plant Physiol.* 153, 34–40.
- Péret, B., De Rybel, B., Casimiro, I., Benková, E., Swarup, R., Laplace, L., Beeckman, T., and Bennett, M.J. (2009). *Arabidopsis* lateral root development: an emerging story. *Trends Plant Sci.* 14, 399–408.
- Péret, B., Li, G., Zhao, J., Band, L.R., Voß, U., Postaire, O., Luu, D.T., Da Ines, O., Casimiro, I., Lucas, M., et al. (2012). Auxin regulates aquaporin function to facilitate lateral root emergence. *Nat. Cell Biol.* 14, 991–998.
- Rinne, P.L., Welling, A., Vahala, J., Ripel, L., Ruonala, R., Kangasjärvi, J., and van der Schoot, C. (2011). Chilling of dormant buds hyperinduces FLOWERING LOCUS T and recruits GA-inducible 1,3-beta-glucanases to reopen signal conduits and release dormancy in *Populus*. *Plant Cell* 23, 130–146.
- Schlereth, A., Möller, B., Liu, W., Kientz, M., Flipse, J., Rademacher, E.H., Schmid, M., Jürgens, G., and Weijers, D. (2010). MONOPTEROS controls embryonic root initiation by regulating a mobile transcription factor. *Nature* 464, 913–916.
- Simpson, C., Thomas, C., Findlay, K., Bayer, E., and Maule, A.J. (2009). An *Arabidopsis* GPI-anchor plasmodesmal neck protein with callose binding activity and potential to regulate cell-to-cell trafficking. *Plant Cell* 21, 581–594.
- Stadler, R., Wright, K.M., Lauterbach, C., Amon, G., Gahrz, M., Feuerstein, A., Oparka, K.J., and Sauer, N. (2005). Expression of GFP-fusions in *Arabidopsis* companion cells reveals non-specific protein trafficking into sieve elements and identifies a novel post-phloem domain in roots. *Plant J.* 47, 319–331.
- Swarup, K., Benková, E., Swarup, R., Casimiro, I., Péret, B., Yang, Y., Parry, G., Nielsen, E., De Smet, I., Vanneste, S., et al. (2008). The auxin influx carrier LAX3 promotes lateral root emergence. *Nat. Cell Biol.* 10, 946–954.
- Swarup, R., Kargul, J., Marchant, A., Zadik, D., Rahman, A., Mills, R., Yemm, A., May, S., Williams, L., Millner, P., et al. (2004). Structure-function analysis of the presumptive *Arabidopsis* auxin permease AUX1. *Plant Cell* 16, 3069–3083.
- Thomas, C.L., Bayer, E.M., Ritzenthaler, C., Fernandez-Calvino, L., and Maule, A.J. (2008). Specific targeting of a plasmodesmal protein affecting cell-to-cell communication. *PLoS Biol.* 6, e7.
- Traas, J., and Vernoux, T. (2010). Plant science. Oscillating roots. *Science* 329, 1290–1291.
- Truernit, E., and Sauer, N. (1995). The promoter of the *Arabidopsis thaliana* SUC2 sucrose-H<sup>+</sup> symporter gene directs expression of beta-glucuronidase to the phloem: evidence for phloem loading and unloading by SUC2. *Planta* 196, 564–570.
- Van Norman, J.M., Breakfield, N.W., and Benfey, P.N. (2011). Intercellular communication during plant development. *Plant Cell* 23, 855–864.
- Vanneste, S., De Rybel, B., Beeckman, T., Ljung, K., De Smet, I., Van Isterdael, G., Naudts, M., Iida, R., Gruijsem, W., Tasaka, M., et al. (2005). Cell cycle progression in the pericycle is not sufficient for SOLITARY ROOT/IAA14-mediated lateral root initiation in *Arabidopsis thaliana*. *Plant Cell* 17, 3035–3050.
- Vatén, A., Dettmer, J., Wu, S., Stierhof, Y.D., Miyashima, S., Yadav, S.R., Roberts, C.J., Campilho, A., Bulone, V., Lichtenberger, R., et al. (2011). Callose biosynthesis regulates symplastic trafficking during root development. *Dev. Cell* 21, 1144–1155.
- Xu, X.M., and Jackson, D. (2010). Lights at the end of the tunnel: new views of plasmodesmal structure and function. *Curr. Opin. Plant Biol.* 13, 684–692.
- Xu, X.M., Wang, J., Xuan, Z., Goldshmidt, A., Borrill, P.G., Hariharan, N., Kim, J.Y., and Jackson, D. (2011). Chaperonins facilitate KNOTTED1 cell-to-cell trafficking and stem cell function. *Science* 333, 1141–1144.
- Zavaliev, R., Ueki, S., Epel, B.L., and Citovsky, V. (2011). Biology of callose ( $\beta$ -1,3-glucan) turnover at plasmodesmata. *Protoplasma* 248, 117–130.